

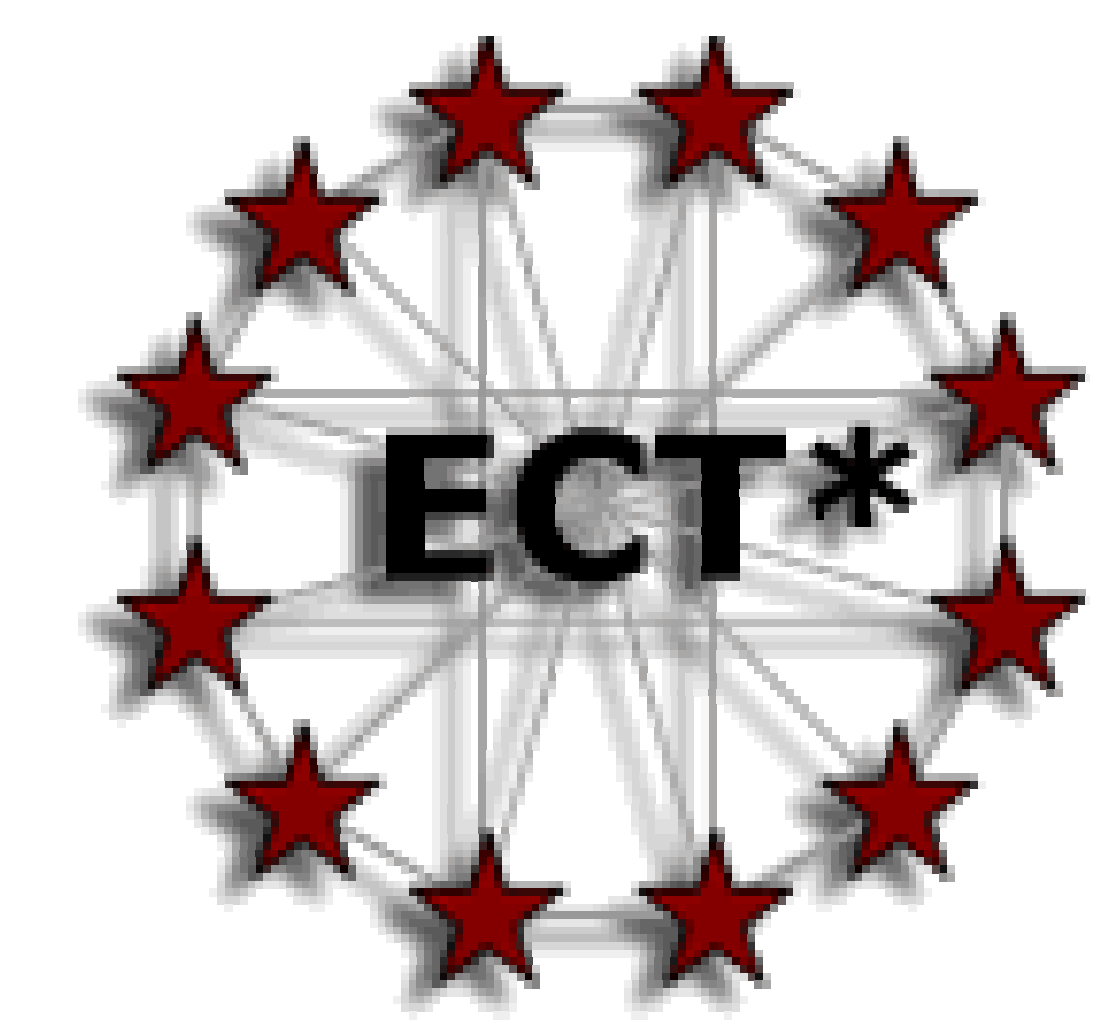
Order-to-chaos transition in the Geometric Collective Model using Geometric Criteria

Pavel Stránský^{1,2,*}, Pavel Cejnar²

¹European Centre for Theoretical Studies in Nuclear Physics and Related Areas (ECT*), Strada delle Tabarelle 286, I-38123 Villazzano, Trento, Italy

²Institute of Particle and Nuclear Physics, Faculty of Mathematics and Physics, Charles University, V Holešovickách 2, CZ-18000, Prague, Czech Republic

*email@pavelstransky.cz



ABSTRACT: A method of differential geometry is applied to study the transition between regular and chaotic dynamics in the classical version of the Geometric Collective Model of atomic nuclei. The Hamiltonian of the system is expressed in terms of the curvature associated with a Riemannian metric tensor and, using a simple algebra without the need of solving differential equations, it is possible to find the energy where unstable motion appears. We show that the geometrical method is in agreement with a careful numerical analysis of regularity based on the measure calculated from Poincaré sections. It is also observed that the condition of stability corresponds with the changes in the shape of the boundary of the potential at a given energy (kinematically accessible region).

Geometrical method

The theory, recently developed by Horwitz *et al.* [1, 2] demonstrates that every Hamiltonian with the standard kinetic term, and the potential $V(\mathbf{x})$ depending only on space variables, can be transformed to the Hamiltonian corresponding with a free motion in the curved space (this procedure is the so called geometrical embedding of the Hamiltonian motion)

$$H = \frac{1}{2M} \mathbf{p}^2 + V(\mathbf{x}) \quad \rightarrow \quad H' = \frac{1}{2M} g_{ij}(\mathbf{x}) p^i p^j, \quad (1)$$

described by the metric tensor of conformal form

$$g_{ij}(\mathbf{x}) = \frac{E}{E - V(\mathbf{x})} \delta_{ij}, \quad (2)$$

defined on the hypersurface $E = \text{const}$. Then the geodesic motion $\ddot{x}^i = -\Gamma_{jk}^i \dot{x}^j \dot{x}^k$ with the connection form

$$\Gamma_{jk}^i = \frac{1}{2} g^{il} \frac{\partial g_{jl}}{\partial x^i} \quad (3)$$

coincides with the solution of the Hamilton equations of motion of the original flat-space problem (1). Note that the connection form (3) is not compatible with the metric g_{ij} . Nevertheless, it satisfies the requirements for the construction of the covariant derivative

$$\nabla_i \xi^j = \frac{\partial \xi^j}{\partial x^i} + \Gamma_{ik}^j \xi^k. \quad (4)$$

The equation of the geodesic deviation for two neighboring trajectories $\xi^i \equiv x^i - x'^i$ reads as

$$\frac{D^2 \xi^i}{Dt^2} = R_{jkl}^i \frac{dx^j}{dt} \xi^k \frac{dx^l}{dt}, \quad (5)$$

where the symbol D/Dt stands for the covariant derivative along the orbit x^j and R_{jkl}^i is the Riemann curvature tensor associated with the connection form (3). By including the explicit expression for the metric (2) the equation of the geodesic equation becomes $D^2 \xi / Dt^2 = -\mathcal{V} \mathcal{P} \xi$, where

$$\mathcal{V}_{ij} = \frac{3}{M^2 v^2} \frac{\partial V}{\partial x^i} \frac{\partial V}{\partial x^j} + \frac{1}{M} \frac{\partial^2 V}{\partial x^i \partial x^j} \quad (6)$$

is the *stability matrix* and \mathcal{P} is the projector into a direction orthogonal to the velocity \dot{x}^i . Instability should occur if at least one of the eigenvalues of \mathcal{V} is negative.

Geometric Collective Model

The Geometric Collective Model (GCM) [3] describes vibrational and rotational dynamics of quadrupole deformed nuclei. The instantaneous deformation is determined by the Bohr variables β (measuring the deformation size) and γ (characterizing the shape type), being polar coordinates in the plane (x, y) of intrinsic components of the quadrupole deformation tensor (see Fig. 1), while the orientation of the nucleus in the laboratory coordinate system is given by three Euler angles $(\theta_1, \theta_2, \theta_3)$.

The Hamiltonian $H = T_{\text{rot}} + T_{\text{vib}} + V$ in the intrinsic frame consists of the vibrational and rotational kinetic energy, and the potential energy of the deformation. Here we consider only the non-rotational case $T_{\text{rot}} = 0$ and the potential energy up to the quartic term in β

$$T = \frac{1}{2K} (p_x^2 + p_y^2), \quad (7)$$

$$V = A (x^2 + y^2) + Bx (x^2 - 3y^2) + C (x^2 + y^2)^2, \quad (8)$$

where (p_x, p_y) are the momenta conjugated with the coordinates (x, y) and (A, B, C, K) are adjustable parameters. The Hamiltonian can be solved both in classical and quantum mechanics [4]. However, we focus here on the classical solution only. Without the loss of generality, one can rescale in this case the physical units of energy, coordinate and time, and remain with only one fundamental parameter of the model.

It has been shown that the GCM exhibits rather complicated interplay between order and chaos [4] if the external parameter and the energy are varied. In order to quantify classical chaoticity, the fraction of regularity f_{reg} is introduced as the ratio of the phase-space volume filled by regular trajectories to the total volume accessible at a given energy. This ratio can be well approximated by the corresponding ratios on the Poincaré surfaces of section.

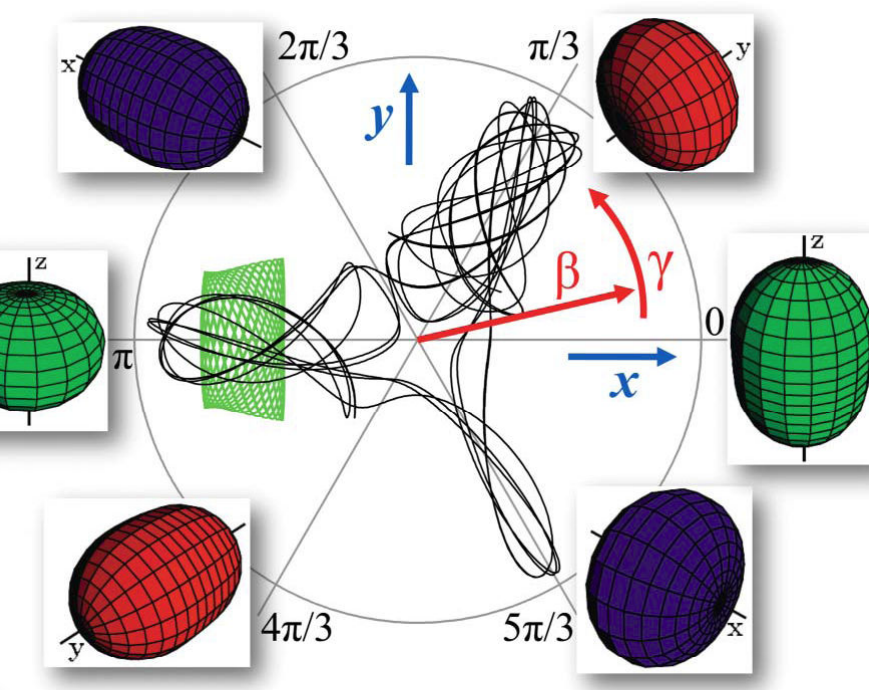


FIGURE 1: The plane of deformation parameters (β, γ) or (x, y) with images of intrinsic shapes. Two classical trajectories at $A = -1, B = 1.09, C = 1$ and $E = 0$ (black and green curve) represent examples of regular and chaotic vibrations.

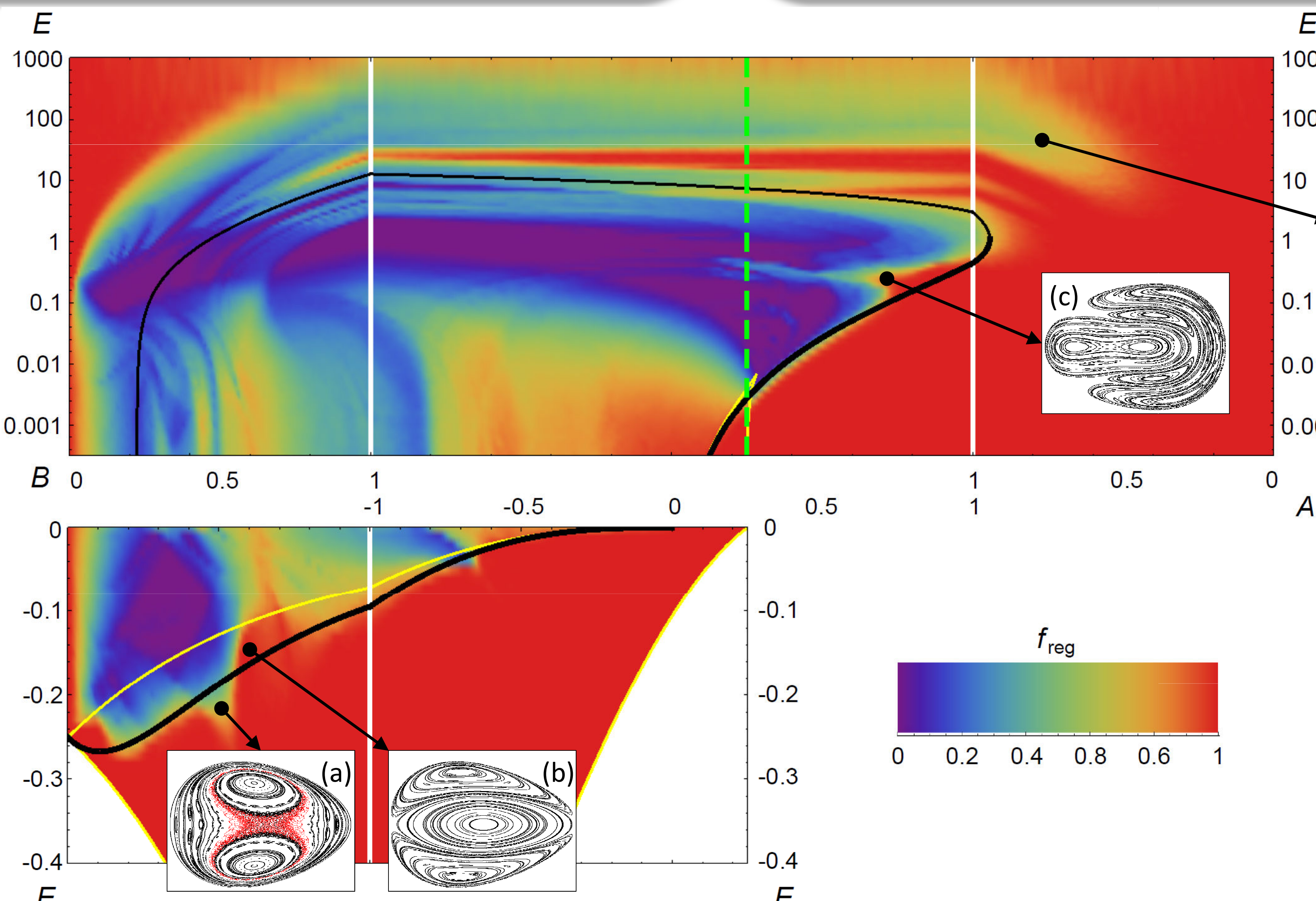


FIGURE 2: Complete map of classical chaos in the GCM, and selected Poincaré sections. The fraction of regularity f_{reg} is coded in colors (red = perfect order, violet = complete chaos). The vertical axis corresponds to the absolute energy (split to parts $E < 0$ in linear scale and $E > 0$ in logarithmic scale). The horizontal axis displays parameters A and B (the parameterization changes at white thick lines). The dashed green line marks the phase transition between deformed and spherical ground-state shapes. **The black line corresponds to the convex-concave (thick lower part) and concave-convex (thin higher part) transition in the shape of the kinematically accessible area.** Note that the lower part equals to the stable-unstable transition determined with the geometrical method. The yellow lines indicate the global minimum and the saddle point ($E < 0$), and the local maximum and minimum ($E > 0$) of the potential. Three selected Poincaré sections are taken from the places of the map where the unstable motion penetrates into the supposedly stable region (panels a, d) or vice versa (panels b, c). Each section shows in total 50 thousand passages of 50 trajectories through the $y = 0$ plane in the phase space (the scales of x and p_x axes are suppressed). Points corresponding with regular (chaotic) trajectories are painted in black (red).

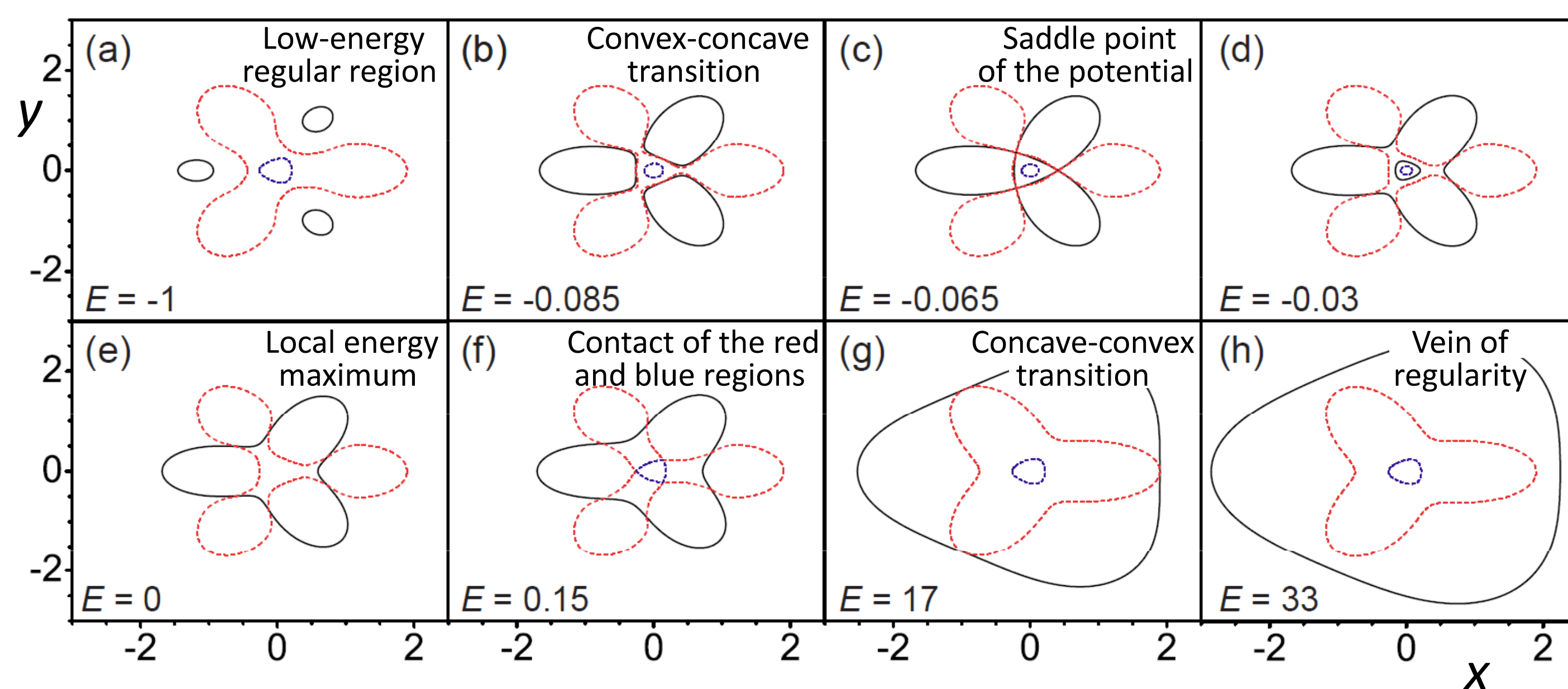


FIGURE 4. Space distribution of the negative eigenvalues of the matrix \mathcal{V} at various energies and at $A = -1, B = 1.09$. The red (blue) dashed line encircles the region where the smaller (larger) eigenvalue is negative. An occurrence of a negative eigenvalue inside the kinematically accessible area (bounded by the black solid curve) indicates the instability of the motion (see Fig. 5). Note that the passage of a negative eigenvalue region through the border of the accessible area makes the border concave.

Results and Discussion

Due to the simplicity of the kinetic term (7), the GCM is suitable for application of the geometrical method. It is possible to solve explicitly at what energy E_t the lower eigenvalue of the stability matrix (6) becomes negative inside the kinematically accessible region

$$E_t = \min_{\pm} \left\{ V \left(x = \frac{6B \pm \sqrt{36B^2 - 32AC}}{8C}, y = 0 \right) \right\}. \quad (9)$$

When $E < E_t$, the stable dynamics should be guaranteed (note that in the very low energy region the potential can be approximated by a quasiperiodic two-dimensional harmonic oscillator), while the diverging areas of negative curvature for $E > E_t$ are the source of instability.

The transitional energy E_t is displayed in Fig. 2 by the thick black curve that follows indeed the frontier of the completely regular dynamics (red color). However, a more detailed inspection reveals that the instability appears slightly below the line (see the Poincaré section of the most pronounced case in panel a), and the geometrical method fails also to predict the instability on the rightmost side of the image. The opposite situation of enhanced regularity inside the regions supposedly unstable is observed as well, the most remarkable being the “veins of regularity” (the red lines in the middle part of Fig. 2); other examples are demonstrated in panels (b), (c). These deviations can be caused by the parametric instability [5], and by the strong stabilizing effect of the regions with positive definite stability matrix.

Another indicator of chaos based on the convexity of the equipotential curves [6] appears to be equivalent, in the case of the GCM, to the geometrical approach. This is depicted in Fig. 4. The part of an equipotential curve that is crossed with a region of negative eigenvalues \mathcal{V} concaves towards the center of the kinematically accessible area.

Conclusions and Outlook

The analytic condition of instability (9) highly approximates the results obtained by the more expensive technique of the fraction of regularity. In addition, since the geometrical method is directly related with the convexity of the potential surface shape, it allows for a very convenient estimate of the stability based only on the visual inspection of the potential. A great advantage of the geometrical method is that it does not require to solve the full system of differential equations of motion, but only the diagonalization of small matrices is necessary. However, the connection between the geometrical method and the instability of trajectories still lacks of a general proof, and both approaches exhibit a small, but nonnegligible difference. This difference, as well as the case of more general kinetic terms, will be addressed to a future work. All the results of this Poster will be summarized and published in [7].

Acknowledgement

The authors highly appreciate many inspiring suggestions and comments of M. Macek, A. Frank, E. Landa, I. Morales, and R. Fossion. Part of this work has been done at Instituto de Ciencias Nucleares, UNAM, Mexico, whose kind hospitality is gratefully acknowledged. This work was partly supported by Czech Science Foundation (grant no. 202/06/0363) and by the Czech Ministry of Education (contracts nos. 0021620859 and LA 314).

References

- [1] L. Horwitz, Y.B. Zion, M. Lewkowicz, M. Schiffer, and J. Levitan, Phys. Rev. Lett. **98**, 234301 (2007).
- [2] Y.B. Zion and L. Horwitz, Phys. Rev. E **76**, 046220 (2007); Phys. Rev. E **78**, 036209 (2008); Phys. Rev. E **81**, 046217 (2010).
- [3] D.J. Rowe and J.L. Wood, *Fundamentals of Nuclear Models* (World Scientific, Singapore, 2010).
- [4] P. Cejnar and P. Stránský, Phys. Rev. Lett. **93**, 102502 (2004); P. Stránský, M. Kurian, and P. Cejnar, Phys. Rev. C **74**, 6342 (2006); P. Stránský, P. Hruška, and P. Cejnar, Phys. Rev. E **79**, 046202 (2009); Phys. Rev. E **79**, 066201 (2009).
- [5] L. Casetti, M. Pettini, and E.G.D. Cohen, Phys. Rep. **337**, 237 (2000).
- [6] J. Li and S. Zhang, Phys. Lett. A **375**, 1710 (2011).
- [7] P. Stránský and P. Cejnar, in preparation.

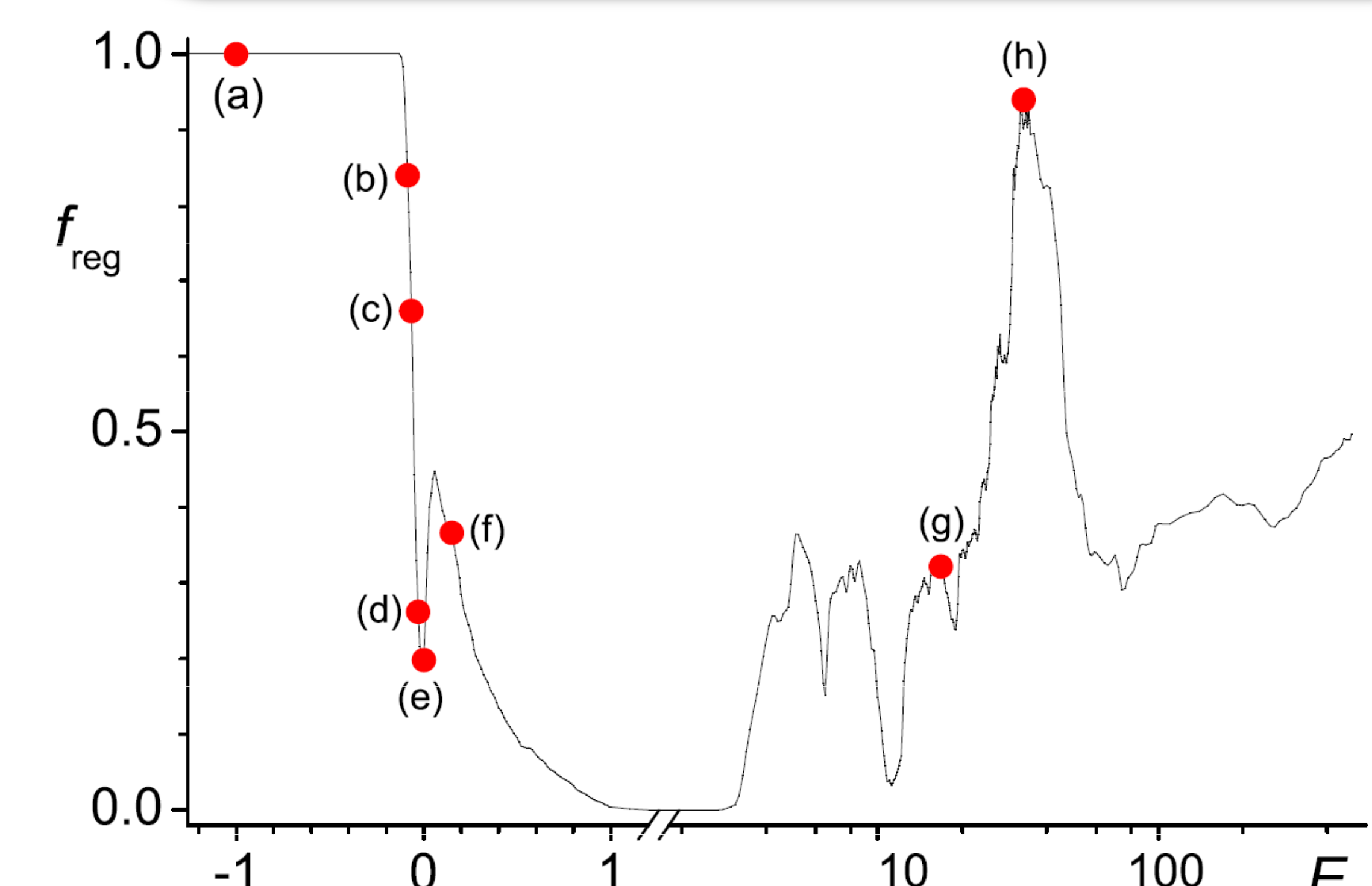


FIGURE 3: f_{reg} dependence on energy E . This figure is a special cut of Fig. 2 at $A = -1$ and $B = 1.09$. The red points show eight distinct energies important for the stable-unstable evolution, discussed in Figs. 4 and 5.

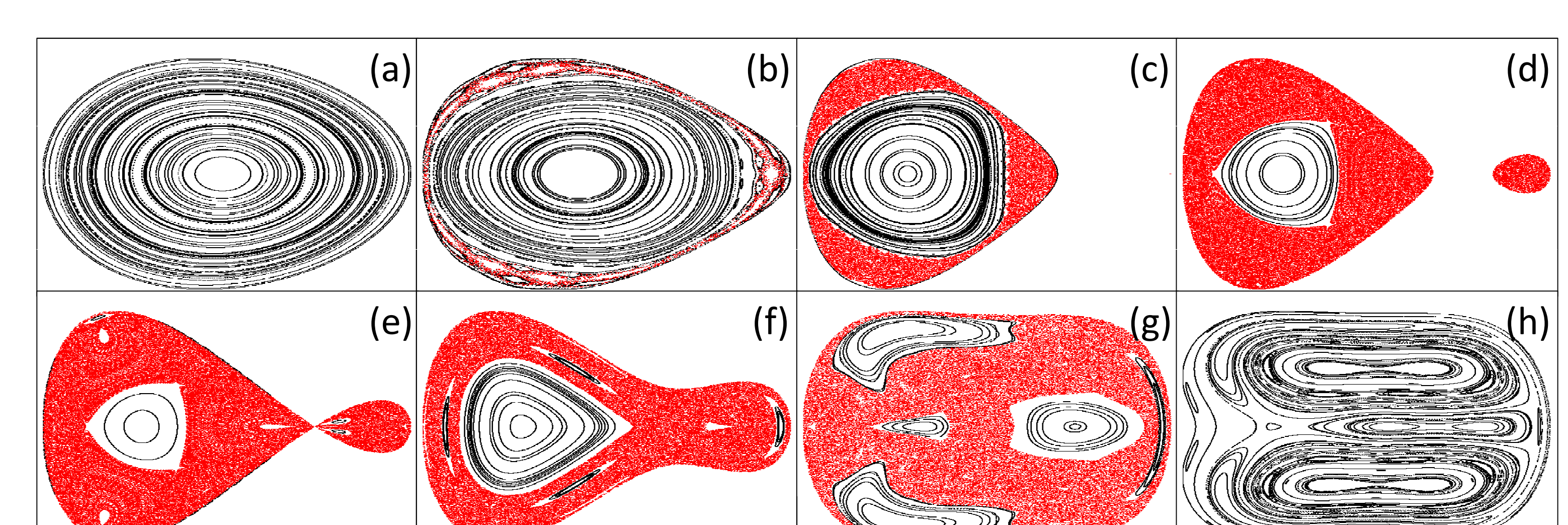


FIGURE 5. Changes in Poincaré sections when passing the convex-concave-convex transition in the boundary of the kinematically accessible region. The labels of the panels correspond to Fig. 3. One observes that deeply in the stable region (panel a, $E = -1$) the motion is fully regular. At the stable-unstable boundary line, a small chaotic region is already present. Panel (g) shows the situation when the border of the kinematically accessible area becomes convex again, however the unstable motion persists due to the permanence of the negative eigenvalues inside. An unexpectedly fully regular motion is observed in panel (h) (see the noticeable “veins of regularity” in Fig. 2).